Acids from fruits generate photoactive Fe-complexes, enhancing solar disinfection of water (SODIS): A systematic study of the novel "*fruto-Fenton*" process, effective over a wide pH range (4 – 9).

Giulio Farinelli [a,*], Stefanos Giannakis [b,*], Aline Schaub [c], Mona Kohantorabi [d], Cesar Pulgarin [b,e,f]

[a] *Institut Européen des Membranes, IEM-UMR 5635, Université de Montpellier, ENSCM, CNRS 34090, Montpellier, France*
[b] *Universidad Politécnica de Madrid, E.T.S. de Ingenieros de Caminos, Canales y Puertos, Departamento de Ingeniería Civil: Hidráulica, Energía y Medio Ambiente, Environment, Coast and Ocean Research Laboratory (ECOREL-UPM), c/Profesor Aranguren s/n 28040, Madrid, Spain*
[c] *School of Basic Sciences (SB), Institute of Chemical Science and Engineering (ISIC), Group of Advanced Oxidation Processes (GPAO), École Polytechnique Fédérale de Lausanne (EPFL), Station 6 CH-1015, Lausanne, Switzerland*
[d] *Center for X-ray and Nano Science (CXNS), Deutsches Elektronen-Synchrotron (DESY), Notkestr. 85, Hamburg 22607, Germany*
[e] *Environmental Remediation and Biocatalysis Group, Institute of Chemistry, Faculty of Exact and Natural Sciences, Universidad de Antioquia, Calle, 70 No. 52–21, Medellín, Colombia*
[f] *Colombian Academy of Exact, Physical and Natural Sciences, Carrera 28 A No. 39A-63, Bogotá, Colombia*

ARTICLE INFO

ABSTRACT

This study aimed to enhance solar disinfection (SODIS) by the photo-Fenton process, operated at natural pH, through the re-utilization of fruit wastes. For this purpose, pure organic acids present in fruits and alimentary wastes were tested and compared with synthetic complexing agents. Owing to solar light, complexes between iron and artificial or natural chelators can be regenerated through ligand-to-metal charge transfer (LMCT) during disinfection. The target complexes were photoactive under solar light, and the Fe:Ligand ratios for *ex situ* prepared iron complexes were assessed, achieving a balance between iron solubilization and competition with bacteria as a target for oxidizing species. In addition, waste extracts containing natural acidic ligands were an excellent raw material for our disinfection enhancement purposes. Indeed, lemon and orange juice or their peel infusions turned out to be more efficient than commercially available organic acids, leading to complete inactivation in less than 1 h by this novel "*fruto-Fenton*" process, *i.e.* in the presence of a fruit-derived ligand, Fe(II) and H_2O_2. Finally, its application in Lake Leman water and *in situ* complex generation led to effective bacterial inactivation, even in mildly alkaline surface waters. This work proposes interesting SODIS and fruit-mediated photo-Fenton enhancements for bacterial inactivation in resource-poor contexts and/or under the prism of circular economy.

1. Introduction

Water scarcity and contamination are two water issues that are tightly correlated (Daoudy et al., 2022; WHO/UNICEF, 2015). The continuous growth of the population worldwide will endanger this finite resource, with exponentially increasing water demand, together with an increase in contaminant concentration in wastewater effluents. In resource-poor contexts, where there is a lack of infrastructure and traditional wastewater treatment plants (WWTP), biological contaminants, including bacteria, viruses, and protozoan parasites, are far more

widespread than chemical contaminants (WHO/UNICEF 2015). Water problems are worsening in these areas. Indeed, it is predicted that close to 230 million Africans will soon face water scarcity, and up to 460 million will be living in water-stressed areas (Daoudy et al., 2022; McGuigan et al., 2012). Household water treatment and storage (HWTS) interventions, such as solar disinfection (SODIS), represent a valid alternative to traditional treatments, such as boiling, chlorination, and filtration, and have gained popularity over the past 10 years (Chaúque and Rott, 2021; García-Gil et al., 2021; Giannakis et al., 2016; Ubomba-Jaswa et al., 2010). Indeed, boiling water requires energy; hence,

firewood, if used on a large scale, will increase deforestation in rural areas where the latter is already a problem. Moreover, disinfection by chlorine compounds is often rejected by consumers because of undesirable tastes and odors; hence, there is a lack of confidence in the proposed drinking water (Wegelin et al., 1994). However, SODIS addresses water disinfection using solar light; hence, UV rays that can kill pathogens trigger intracellular oxidative reactions and genome damage (Cabiscol et al., 2000; Giannakis et al., 2016; Halliwell and Aruoma, 1991; Lloyd et al., 1997; Mitchell et al., 2014; Sinha and Häder, 2002). However, this can be further optimized. In this direction, solar-assisted advanced oxidation processes (AOPs) present great disinfection potential (Clarizia et al., 2017; Coha et al., 2021), since SODIS is the baseline and main enhancement of various AOPs. Specifically, the photo-Fenton process ($Fe^{2+}/H_2O_2/h\nu$), could result in promising applications for resource-poor communities, compared to other AOPs that use complicated equipment and expensive reagents (Fernandes et al., 2020; Mazhar et al., 2020; Polo-López and Sánchez Pérez, 2021; Roccaro et al., 2009; Ruales-Lonfat et al., 2015; Spuhler et al., 2010). This process generates highly reactive hydroxyl radicals according to the following principal reaction (Eq. (1)), with Eq.2 being the bottleneck, the kinetically limiting step in the regeneration of Fe^{3+} to Fe^{2+} (Koppenol, 2001):

$$Fe^{2+} + H_2O_2 \rightarrow Fe^{3+} + OH^- + HO^\bullet \tag{1}$$

$$Fe^{3+} + H_2O_2 \rightarrow Fe^{2+} + HO_2^\bullet + H^+ \tag{2}$$

Irradiation accelerates the process (i.e., the photo-Fenton process), allowing faster regeneration of Fe^{2+} (Giannakis et al., 2016; Spuhler et al., 2010). The process pH was perceived as the limiting factor for photo-Fenton systems because $FeOH^{2+}$, the most photoactive Fe^{3+} hydroxy complex, is predominant at low pH (2.8) (Spuhler et al., 2010) and much lower at higher pH (Ruales-Lonfat et al., 2015; Spuhler et al., 2010). Iron organo-complexes, which absorb light in the solar spectrum and are stable at environmental pH can mitigate the pH dependency of traditional photo-Fenton systems (Ahile et al., 2021; U.J. 2020; De Luca et al., 2014; Gomes Júnior et al., 2018; Papoutsakis et al., 2015). EDTA, EDDS, NTA, citrate, and others have resulted in effective organic ligands in near-neutral photo-Fenton processes (De Luca et al., 2014; Pulgarin et al., 2022; A. 2020; Sun New Haven, CT), where the reduction takes place through ligand-to-metal charge transfer (LMCT) between the organic ligand and iron, with the ligand acting as the sacrificial electron donor (Eq. (3) shows the reaction scheme (Oller et al., 2011; Roca et al., 2011)). Other biodegradable photo-Fenton catalysts reported in the literature act in the same fashion (Fiorentino et al., 2018). One of the products is the oxidized ligand $R^\bullet$, which can react with the dissolved oxygen present in water to produce further ROS according to Eq. (4) (Roca et al., 2011).

$$[Fe(RCOO)]^{2+} + h\nu \rightarrow Fe^{2+} + R^\bullet + CO_2 \tag{3}$$

$$R^\bullet + O_2 \rightarrow O_2^{\bullet-} + CO_2 \tag{4}$$
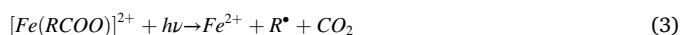
However, synthetic ligands, such as EDTA, EDDS, and NTA, are neither cheap nor easy to access in rural areas and developing countries, and some of these compounds have been identified as harmful (Guilhermino et al., 1997; Ruales-Lonfat et al., 2016). On the other hand, natural ligands such as citric, tartaric, ascorbic, malic, and quinic acids are cheaper than synthetic ones, biodegradable, and potentially easier to access in developing countries, but their pure forms may still be difficult to find in those areas. Fortunately, the fruits contain natural ligands. Fruits and their parts are cheaper and easier to obtain than pure chemicals and are one of the major by-products of the food industry. For instance, in South Africa, 44 % (by mass) of food waste consists of fruits and vegetables (Nahman and de Lange, 2013).

The idea of using agro-industrial by-products to enhance an existing process is in line with current global issues, such as overproduction and overconsumption in industrialized countries, along with the lack of

resources in developing countries (Manrique-Losada et al., 2022). Citrus fruits are particularly rich in organic acids, which have been assessed previously, and effectively enhance the photo-Fenton process in various contexts (Villegas- Guzman et al., 2017). According to Flores et al., 2.4 g of organic acids per 100 g of fruit weight (FW) are present in oranges; hence, citric acid (CA), malic acid (MA), glutamic acid (GA), and quinic acid (QA) are also found (91.3 wt%, 5.8 wt%, 2.2 wt%, 0.6 wt%, respectively) (Flores et al., 2012). Also, in lemon 5.5 g of organic acids for 100 g FW, hence citric acid, malic, glutamic, and quinic acids are present (93.6 wt%, 4.1 wt%, 1.4 wt%, 0.8 wt%, respectively) (Flores et al., 2012). Ascorbic acid (AA) is also found in citrus fruits (Scherer et al., 2012). Other than citric acid, other organic compounds, such as flavonoids or tannic acids, may also play a role in the LMCT process; however, citric acid is the predominant complexing agent in lemons and oranges (García-Ballesteros et al., 2016). It is now clear that there is an untapped resource that can potentially enhance SODIS in a bio-compatible way while moving towards the direction of sustainable reuse of resources.

This work developed an applicable procedure to efficiently use organic acids from fruit by-products and promote LMCT for the enhancement of the photo-Fenton process to kill pathogens in drinking water in resource-poor contexts. This study presents a systematic comparison of different ligands and their iron complexes with insights into their molecular structures and roles in improving their bacterial disinfection capacity. First, characterization of the photoactivity of the complexes is provided and explained via the ligand conditional binding constant Kf' at different pH values (i.e., 3 and 7). Furthermore, the investigation shows improved disinfection results of the solar "*fruto-Fenton*" process (from the Greek: "φρούτο" = fruit) with LMCT, using ex-situ prepared ligands with pure forms of natural organic acids (CA, AA, TA, GA, QA, MA), synthetic ligands (EDTA, NTA, EDDS), or directly the pure fruit juice and their peels extract as source of organic acids ligands. Finally, validation by disinfection of *E. coli*-spiked alkaline Lake Leman (surface) water occurred effectively, even with in-situ ligand preparation, mild reagent addition, and moderate temperature/irradiation conditions.

2. Materials and methods

2.1. Chemicals

Etylenediaminetetraacetic acid (EDTA), Ethylenediamine-N,N'-disuccinic acid (EDDS), and Titanium(IV) oxysulfate solution 1.9–2.1 % were purchased from Fluka. Sodium hydroxide 0.1 M was supplied by Riedel de Haën. All other chemicals used in this study were purchased from Sigma-Aldrich. MilliQ water (Millipore Elix Advantage 3, Millipore AG) is used for the preparation of the aqueous solutions (15.8 MΩ cm).

2.2. Analytical methods

A UV–VIS spectrophotometer (UV-1800, Shimadzu) was used to measure the absorbance spectra of the complexes at different pH values and ratios to determine the photoactivity of the iron-acid complexes. A total organic carbon analyzer (TOC-V$_{CSN}$, Shimadzu) equipped with an automatic sample injector (ASI-V, Shimadzu) was used for TOC measurements. The evolution of the iron concentration during bacterial inactivation was measured using the ferrozine method, and the absorbance was recorded at 562 nm (Viollier et al., 2000). The measurement of the concentration of H_2O_2 consisted of 20 μL of titanium (IV) oxysulfate added to 1 mL of sample and the absorbance was recorded at 410 nm; the detection limit of this method is 0.1 mg/L (Ruales-Lonfat et al., 2016) (according to Regulation (EU) 528/2012 concerning the making available on the market and use of biocidal products, a lower amount than 0.1 mg/L of H_2O_2 is considered acceptable for drinking water).

2.3. Microbial methods

All disinfection experiments are carried out using wild-type *Escherichia coli* strain K12 (Deutsche Sammlung von Mikroorganismen und Zellkulturen, DSMZ No. 498) as model bacterial species. This strain is non-pathogenic and allows for a good approximation of fecal indicator bacteria. *E. coli* strain storage is assured in cryo-vials containing 20 % glycerol at −20 °C (replaced yearly). Bacterial pre-cultures were obtained by spreading 20 μL of the strain onto Plate Count Agar (PCA; Merck), followed by 24 h incubation at 37 °C (Heraeus Instruments). A grown colony was then re-plated and spread on a new PCA-containing Petri dish and incubated for an additional 24 h at 37 °C. This 48-h process results in a "mother plate, " which is stored at 4 °C and can be used for approximately two weeks.

To prepare the bacterial stock solution from the master plate, Luria-Bertani (LB) broth was prepared (10 g tryptone, 5 g yeast extract, and 10 g NaCl in 1 L distilled water), followed by autoclaving (15 psi, 121–124 °C, 15 min). A colony from the master plate was inoculated into a sterile flask containing sterilized LB broth. Bacterial growth was performed as previously described by Giannakis et al. (2022). Briefly, *E. coli* grown overnight, reaching their stationary phase, were centrifuged and washed twice with sterile saline solution (0.8 % NaCl and 0.08 % KCl), with a final (stock) concentration of approximately 10^9 CFU/mL. Appropriate dilutions were obtained before experimentation in water (10^6 CFU/mL starting concentration).

Bacterial population evolution was monitored, with 1-mL samples regularly withdrawn and spread-plated on PCA medium. Before plating, the samples were properly diluted to ensure measurable counts of colonies (ideally 15–150 colonies per plate). Colony-forming units were manually counted after 24 h of incubation at 37 °C. This method resulted in a detection limit of 10 CFU/mL for the undiluted samples.

2.4. Experimental setup

The experiments were run by ensuring simulated solar light exposure with a bench-scale solar simulator (Suntest CPS, Hereaus), employing a 1500-W air-cooled xenon lamp with infrared and UV-C cut-off filters. The light intensity applied within the experiments (700–900 W/m^2) was monitored using a pyranometer and corresponds to daylight intensity in the areas candidate for SODIS (Samoili et al., 2022). The 700 and 900 W/m^2 irradiance values refer to the global irradiance measured by the pyranometer in the > 300 nm range. This includes a large portion of UVB and all UVA wavelengths. The solar simulators used in this study can be equipped with different combinations of filters to simulate extreme, natural daylight and indoor conditions. This study used the daylight combinations and the 700–900 W/m^2 ranged from 27.6 ± 2.3 to 36.1 ± 1.8 W/m^2 UV in the 290–390 nm range measured by a pyranometer. These values were in the range of 24–36 W/m^2, close to the range encountered in Almeria, south of Spain, during the summer (Attar et al., 2023; Gualda-Alonso et al., 2022; Pichel et al., 2023). Before each experimental run, the reactors were sterilized by autoclaving (FVG3, Fedegari Autoklaven AG). After each experiment, the reactors were washed using acid to ensure iron removal, ethanol to remove any other contaminants, and finally, rinsed with abundant quantities of deionized water.

In lake water experiments, an intensity of 700 W/m^2 was selected to delineate the contribution of the ligand-mediated process to bacterial inactivation, with less pronounced solar effects. The experiments were conducted by placing 500-mL plastic (PET) bottles in a water-cooled bath containing *E. coli*-spiked, unprocessed Lake Leman water (withdrawn at St. Sulpice Water Treatment Station, Switzerland).

2.5. Experimental strategy

The experiments were performed using Milli-Q water and lake water. In the MilliQ water experiments, 100 mL of water containing approximately 10^6 CFU/mL of E. coli was prepared and exposed to various experimental conditions by changing the iron:ligand ratio (Fe:L, 1:1, 1:2, and 1:5) and the type of organic ligand. Note that an iron:ligand ratio of 1:5 was chosen to evaluate the eventual beneficial or detrimental role of the ligand radical formed during the LMCT mechanism, but it was not chosen to optimize the stability of the complex. The Fe:L complexes were prepared *ex situ* (i.e., in a separate graduated flask) by mixing an iron and ligand solution for 5 min (Farinelli et al., 2020), using an iron concentration of 1 mg/L. The complex was subsequently added to the reactor along with bacteria and H$_2$O$_2$ (Scheme 1a). The Fe:L ratio is intended as a molar ratio with the molarity of the ligands computed with respect to 1 mg/L of iron ions, unless otherwise stated. Ten mg/L of H$_2$O$_2$ were added to each experiment. The pH was measured before (with only the ligand) and at the end of each experiment (after two-hour inactivation by the photo-Fenton process, *vide infra*). Lake water tests were executed with both *ex situ* prepared Fe:L (as previously mentioned) and *in situ* formed ligands. In the latter case, L and Fe were directly mixed in the reactor with lake water, followed by the addition of bacteria and H$_2$O$_2$ to the same reactor (see Scheme 1b).

Furthermore, in the lake water experiments, fruit (lemon and orange) juice and their peel infusions were used instead of an iron ligand. The calculations to determine the correct quantity of juice or infusion to dose in the reactor to obtain an Fe:L concentration of 1:2 are explained in Eq. (5) and 6. For simplicity, citric acid was used as the reference ligand for the calculations. Table 1 lists the results of the calculations. The computed amount of fruit juice or infusion was added to the solution as described in the *ex situ* process, replacing the ligand of synthetic origin.

$$\frac{TOC_{citric\ acid\ in\ juice}}{TOC_{citric\ acid\ "1:2"}} = \frac{TOC_{juice} \cdot \%_{citric\ acid\ in\ fruit}}{TOC_{citric\ acid\ "1:2"}} = Dilution\ factor \qquad (5)$$

$$Volume\ to\ add\ into\ the\ reactor = \frac{Volume\ reactor}{Dilution\ factor} \qquad (6)$$

Fruit juice was obtained by compression of the lemon and orange halves. The peel extract was obtained by boiling the peels of the two oranges or two lemons for 30 min in 1 L of water. The application of fruit peels is convenient compared to that of fruit juice because peels are food waste that can be recycled rather than disposed of.

3. Results and discussion

3.1. Iron-ligand photoactivity

To understand the occurrence of an LMCT process under irradiation, it is crucial to gain insights into the evolution of the elements to be employed, namely their photoactivity. In this study, we used iron ions and their complexes with organic ligands to promote bacterial disinfection in the presence of H$_2$O$_2$ under simulated sunlight (900 W/m^2). Therefore, it is important to understand the photoactivity of the singular elements, namely iron ions, ligands, as well as their complexes. First, the absorbance of solutions of Fe(II) and Fe(III) at 5 mg/L was measured (only for the absorbance tests, see S1a, b in the Supplementary Information (SI)). Both the ions were photoactive in the region between 250 and 550 nm. Furthermore, by increasing the pH, the spectra of Fe(II) increased and the Fe(III) spectra decreased; hence, Fe(II) hydroxides were more photoactive, while Fe(III) hydroxides were less photoactive. In addition, the absorbance of the ligand solution was investigated, and all the ligands absorb between 200 and 300 nm (see S1c, d in the SI). AA and TA exhibited the highest absorbance. Indeed, these two ligands have the highest ability to stabilize the electron; hence, the radical species, owing to more stable resonance structures compared to the others (Clark et al., 2007; Pan et al., 2013) (see S2 in the SI for further details). Therefore, the following investigations will focus more on AA, TA, and CA, but investigate the GA, QA, and MA complexes. CA serves as a reference, being the most studied in the literature and the most

a) *Ex situ* complex preparation

b) *In situ* complex preparation
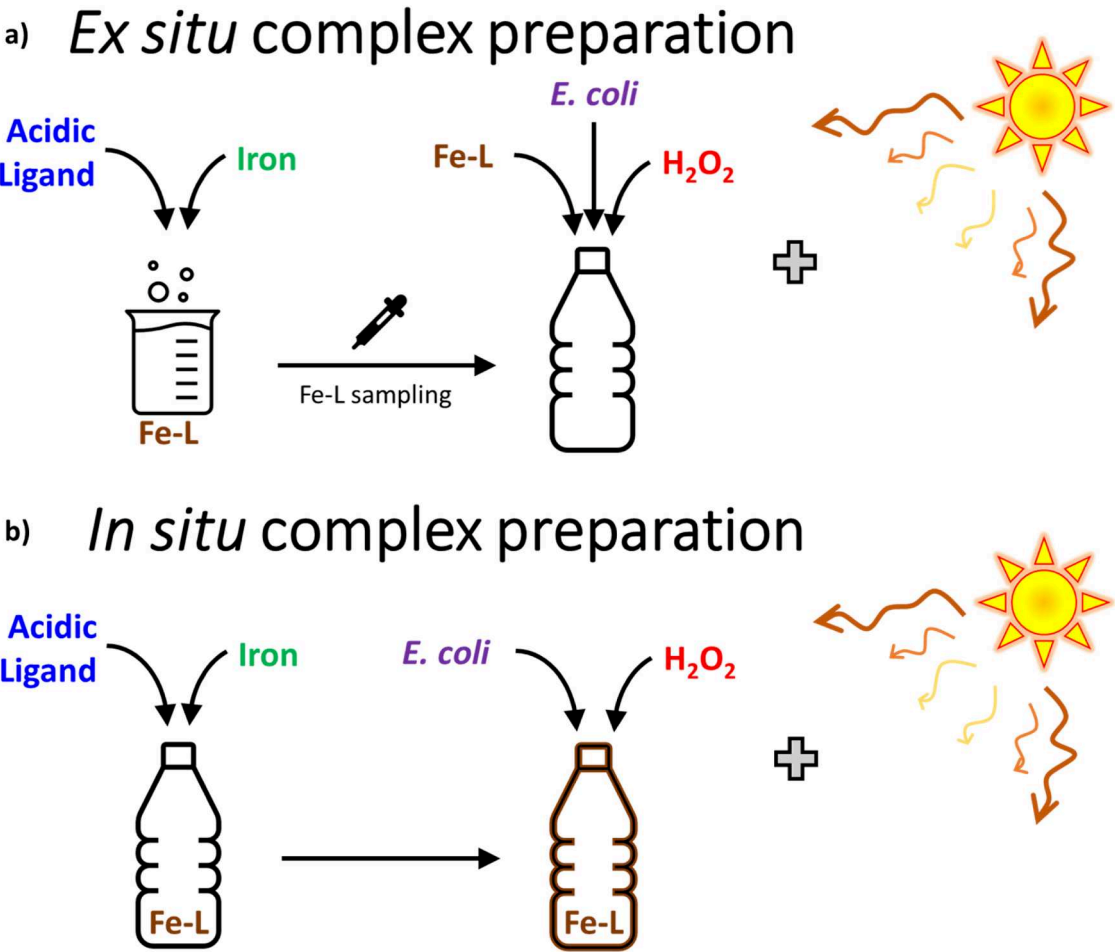
Scheme 1. Preparation, process, and experimental setup of each preparation and experimentation condition.

Table 1
Calculations of juice quantities added to the reactor.

	Citric acid content [%][38]	TOC juice (or infusion) [mg/L]	TOC citric [mg/L]	Dilution factor	Reactor volume [mL]	Volume to add [mL]
Lemon juice	92	1434	1319.24	126.61	100	0.790
Orange juice	90.37	1221	1103.39	105.89	100	0.944
Lemon infusion	92	784	721.28	68.03	100	1.47
Orange infusion	90.37	773	698.56	68.03	100	1.47

abundant in fruits (Pulgarin et al., 2020; Ruales-Lonfat et al., 2016; Seraghni et al., 2012). The complexes with the first three ligands were studied with both Fe(II) and Fe(III) at different molar ratios (1:1, 1:2, and 1:5) and pH values (5, 6, 7, and 8) (see Fig. 1). All other complexes were observed only at pH 7 with an Fe(II,III):Ligand ratio of 1:1 (see Fig. 2).

Fig. 1 shows a 3D plot of the absorbance at a specific wavelength as a function of pH and iron:ligand (Fe:L) ratio. The wavelength selected was the one where the highest absorbance of the species was observed. For the CA and TA complexes, the absorbance tended to increase with increasing pH, while the Fe:L ratio did not have a significant effect. Consistent with the absorbances detected in Figure S1a, b at high pH (7 and 8), the Fe(II) complexes absorb more than those with Fe(III), and the opposite occurs at lower pH values (5 and 6). The same inversion does not occur in the case of AA complexes, likely because of the predominant influence of AA on the absorbance, independent of the central metal. On the other hand, the Fe:L ratio had a significant influence on the AA complexes for both Fe(II) and Fe(III). This is due to the free ascorbic acid present at a high ratio, and its higher ability, compared to the other

ligands, to stabilize an excited state or radical forms, resulting in higher absorbance (Pan et al., 2013).

Fig. 2 shows that all complexes were more photoactive in the UVB and UVA regions. However, they also exhibit photoactivity in the visible range. Specifically, the Fe(II) complexes had a higher absorbance than those with Fe(III) in all cases. Nevertheless, all complexes can absorb solar irradiation and may be used for SODIS enhancement. However, the key to the successful application of ligand-mediated enhancement would be to employ containers with as high UV transparency as possible, since the visible light absorption of the complexes is very weak (García-Gil et al., 2020; Ozores Diez et al., 2020).

Along with the absorbance of the complexes, their quantum yield is an important parameter to gain insights into the relative ability of the ligand to transfer the charge to iron. According to the literature, the quantum yield of the target complexes range from 0.25 to 0.91, and is widely influenced by pH, stoichiometry, and the quality of the matrix. (Abida et al., 2006; Abrahamson et al., 1994; Kocot et al., 2006; Li et al., 2010; Šima and Makáňová, 1997) Since this study aim to evaluate the ability of extracts of fruit waste to enhance SODIS and not the ability of
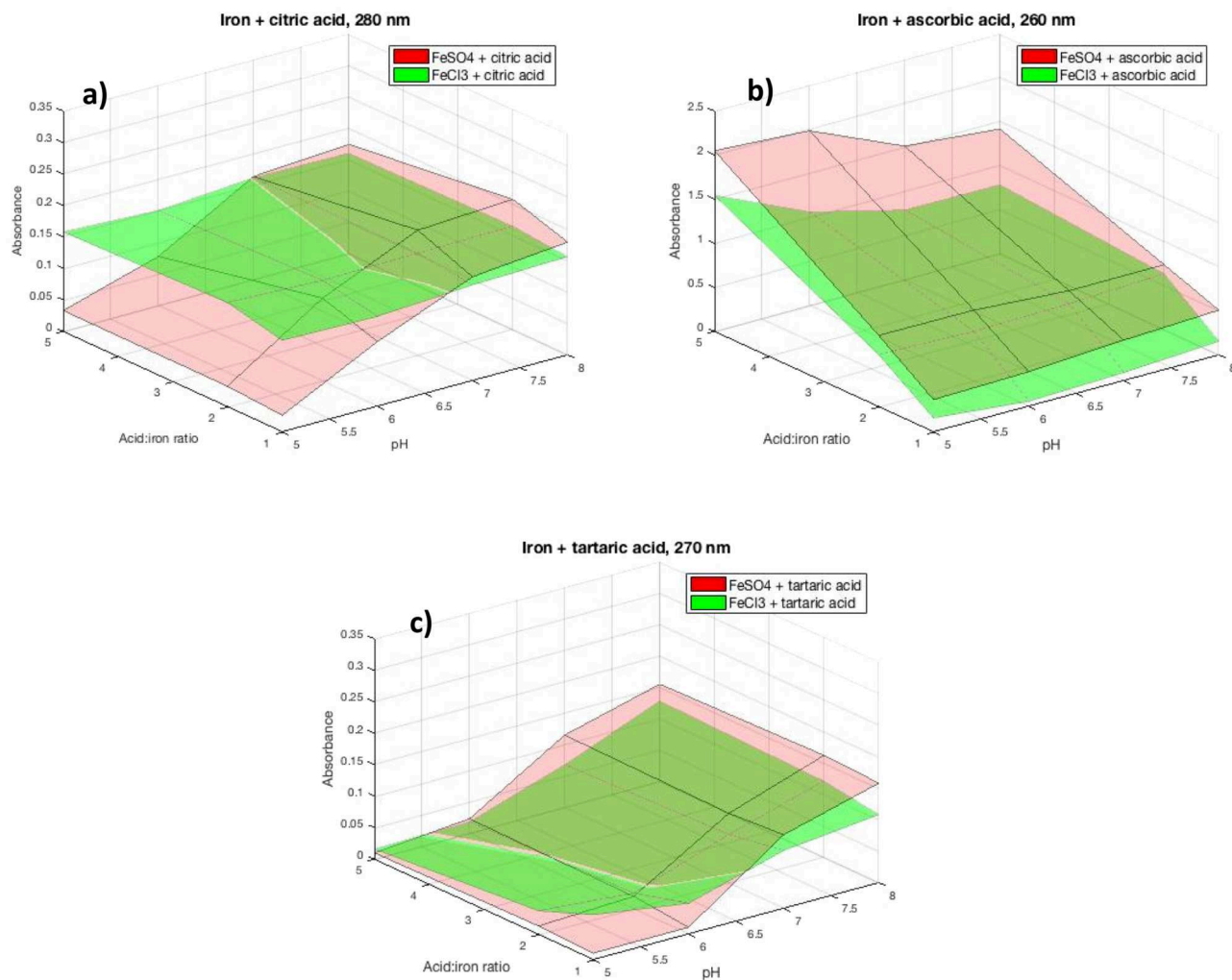
Fig. 1. 3D plots of the absorbance as a function of pH and the Fe:L molar ratio for the three complexes with iron(II) and iron(III). A) iron-citric acid; B) iron-ascorbic acid; and C) iron-tartaric acid. $[Fe^{2+,3+}] = 5$ mg/L.
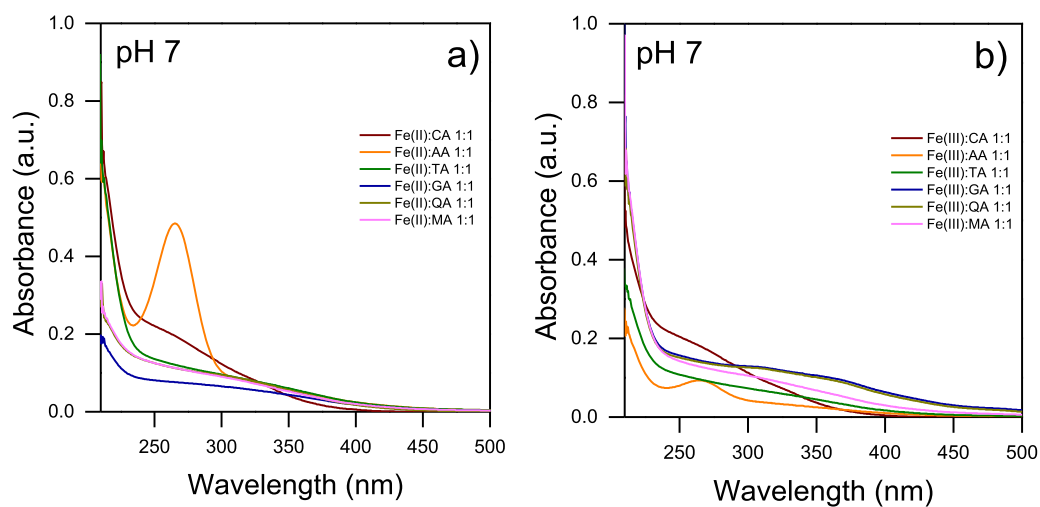

Fig. 2. Absorbance spectra for A) Fe(II)-ligand and B) Fe(III)-ligand complexes at pH 7 with a 1:1 molar ratio. $[Fe^{2+,3+}] = 5$ mg/L; The notation CA, AA, TA, GA, QA, MA is for citric acid, ascorbic acid, tartaric acid, glutamic acid, quinic acid, and malic acid respectively.

the ligands to lead LMCT, a holistic assessment of the relationship between the quantum yield and all the reaction parameters is not presented here.

3.2. Insights into the ligand's conditional binding constant (Kf') and LMCT mechanism

When a catalytic process occurs through an organometallic species, it is also important to evaluate the thermodynamics of the interaction between the central metal and its organo-ligand, and hence, its conditional binding constant (Kf'). Kf' is the force constant of the complexes depending on the pH of the solution and is strictly correlated to the pKa of the target ligand (Farinelli et al., 2020). Fig. 3 shows the Kf' values of the Fe(II) complexes at pH 3 and 7. Fe(II) was selected as the reference central ion because photoactivity experiments provided the most promising results for the latter. Kf' values were computed as described in the SI (Supplementary Text S1). The synthetic ligands (EDTA, EDDS, NTA) showed the highest ability to complex iron at pH 7, but the strength of the EDTA and EDDS complexes decreased at lower acidic pH values. AA resulted in the ligand with the minor ability to stabilize Fe(II) in solution. However, despite their generally lower ability to complex iron, natural ligands are less susceptible to the pH of the solution. This makes the natural ligand complexes more versatile in varied environments and, hence, potentially more applicable.

Insight into the strength of the complex in solution is extremely important to elucidate the ability of the ligand to perform electron transfer. Indeed, it is reasonable to imagine a dichotomy between the ability of the ligands to maintain iron in solution and their ability to stabilize the radical species hence, to perform LMCT. Fig. 4 shows a plausible schematic representation of bacterial inactivation pathways in the presence of ligands.

The ligands facilitate the photo-Fenton reaction as they are photoactive under solar light and initiate several Fenton-related actions (Giannakis et al., 2016). Fig. 4 shows that the mechanism of reduction includes the superoxide/hydroperoxide radical formation ($O_2^{\bullet-}/HO_2^{\bullet}$) and H_2O_2 which can further synergically initiate the photo-Fenttowardsard bacterial inactivation (Giannakis et al., 2016; Pulgarin et al., 2020; Ruales-Lonfat et al., 2016).

There are two mechanisms of iron regeneration under light: via either an inner or an outer electron transfer mechanism (Cieśla et al., 2004). First, $[Fe^{3+}-L_n]$ is excited to the $[Fe^{3+}-L_n]^*$ state, and i) via the inner-sphere mechanism, $L^{\bullet+}$ is formed, and $[Fe^{2+}-L_{n-1}]$; in reaction with another ligand and oxygen, the parent $[Fe^{3+}-L_n]$ is regenerated, or ii) via an electron donor (which gets oxidized) and the reaction of $[Fe^{2+}-L_n]$ with molecular oxygen (Cieśla et al., 2004). Solar light is sufficiently energetic to overpass the ligand-to-metal charge transfer (LMCT) band only if the organic ligand is easily oxidized, thus easily stabilizing the radical form. The one-electron oxidation of the bidentate ligand generated within the process requires a second electron transfer to return to stable oxidation states, which can react either by a) with the parent Fe^{3+}-L complex, b) with oxygen, creating a superoxide radical anion, or c) with other oxidants in the matrix (Cieśla et al., 2004; Šima and Makáňová, 1997). The unstable superoxide radical anions lead to H_2O_2 formation or induce a reduction that can cause biological damage. Therefore, it is clear that the ligand plays an important role in facilitating the catalytic photo-Fenton cycle, initiating additional pathways towards bacterial inactivation (Chaúque and Rott, 2021; Giannakis et al., 2016). The correlation between the Kf' of the complexes and their inactivation efficacy was further underlined in this study.

3.3. Bacterial inactivation with natural ligands

Fig. 5a and b show preliminary tests to understand the best operating conditions in terms of central ions and Fe:L ratio, compared with SODIS and classic photo-Fenton efficacies. In agreement with the literature, Fig. 5a shows the photo-Fenton (and photo-Fenton-like) processes with both Fe(II) and Fe(III), leading to a faster inactivation compared to their constituents. In addition, the process with only Fe(II) is faster than that with Fe(III), which is likely due to the ease of the Fenton reaction when Fe(II) diffuses through the cell because iron already has the oxidation state required for the Fenton reaction (Eq. (1)) (Braun, 2001). In line with this, Fe(III) is not able to diffuse through the cell membrane but requires specific transport mechanisms (Giannakis et al., 2016; Mey et al., 2021). Therefore, Fe(II) was selected as the central ion for the subsequent experiments.

Fig. 5b aims to define the best Fe:L ratio using AA as a reference ligand. The graph shows that when only the ligand was present, a clear decrease in the inactivation rate occurred with an increase in the Fe:L ratio. This indicates that the organic ligand competes with the reaction between bacteria and reactive oxygen species (ROS). Conversely, H_2O_2 enhanced the kinetics of inactivation with a concomitant increase in the Fe:L ratio, facilitating the ligand-enhanced photo-Fenton process. This behavior can be explained by an LMCT mechanism, which helps in the recycling of Fe(II) from Fe(III) while simultaneously maintaining the ions in solution. Therefore, the ligand plays a dual role in iron recycling and solubilization; hence, a higher amount than the ligand is required. This agrees with the explanation proposed by de Luca et al., who suggested that the supplementary ligands allow to avoid iron precipitation (De Luca et al., 2014). Figure S3 in the SI also shows AA as an example and further confirms the beneficial contribution of higher amounts of ligands in the presence of H_2O_2. Figure S3a shows lower residual H_2O_2 concentrations with 1:2 and 1:5 ratios; hence, its higher consumption and higher Fenton activity indiscriminately targeted bacteria and ligands. Likewise, the residual dissolved iron concentration (Figure S3b in SI) is higher when increasing the amount of ligand, due to the AA complexation, which keeps more iron ions in solution available for the Fenton reaction, which in turn leads to faster inactivation. The optimum balance between ligand consumption by ROS and enhanced bacterial inactivation lies in a 1:2 Fe:L ratio in the presence of H_2O_2. Therefore, this ratio was chosen for subsequent experiments.

Fig. 5c shows the results of the inactivation tests with iron ligand complexes in the absence of H_2O_2. Overall, the complexes only marginally enhanced inactivation compared to the standard process (only Fe^{2+}). Meanwhile, Fig. 5d describes the ligand-mediated photo-Fenton process, and Fig. 5 in its entirety, shows that the ligands have a great influence on the inactivation performance when dosed at the optimum ratio. An efficient LMCT process requires both dissolved free iron and ligands in solution to allow multiple synergistic disinfection mechanisms, as shown in Fig. 4 (Giannakis et al., 2016). In this respect, the iron ions need ligands to remain in solution at near-neutral pH; hence, the ligand should have an adequate Kf' to stabilize iron. Conversely, LMCT requires a free ligand in solution to allow recycling of Fe(II) during the Fenton process through its radical structure (Giannakis et al., 2016). Therefore, the ligand cannot create a too strong interaction with iron otherwise it will not be free in solution, and at the same time, its structure should be able to stabilize the radical to persist in solution
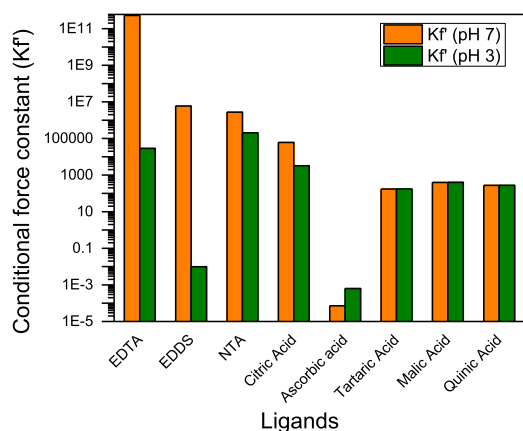

Fig. 3. Kf' computed at pH 7 and 3 for a variety of complexes with Fe(II). See SI for the computing procedure. Please note that data related to glutamic acid were not available in the consulted database.
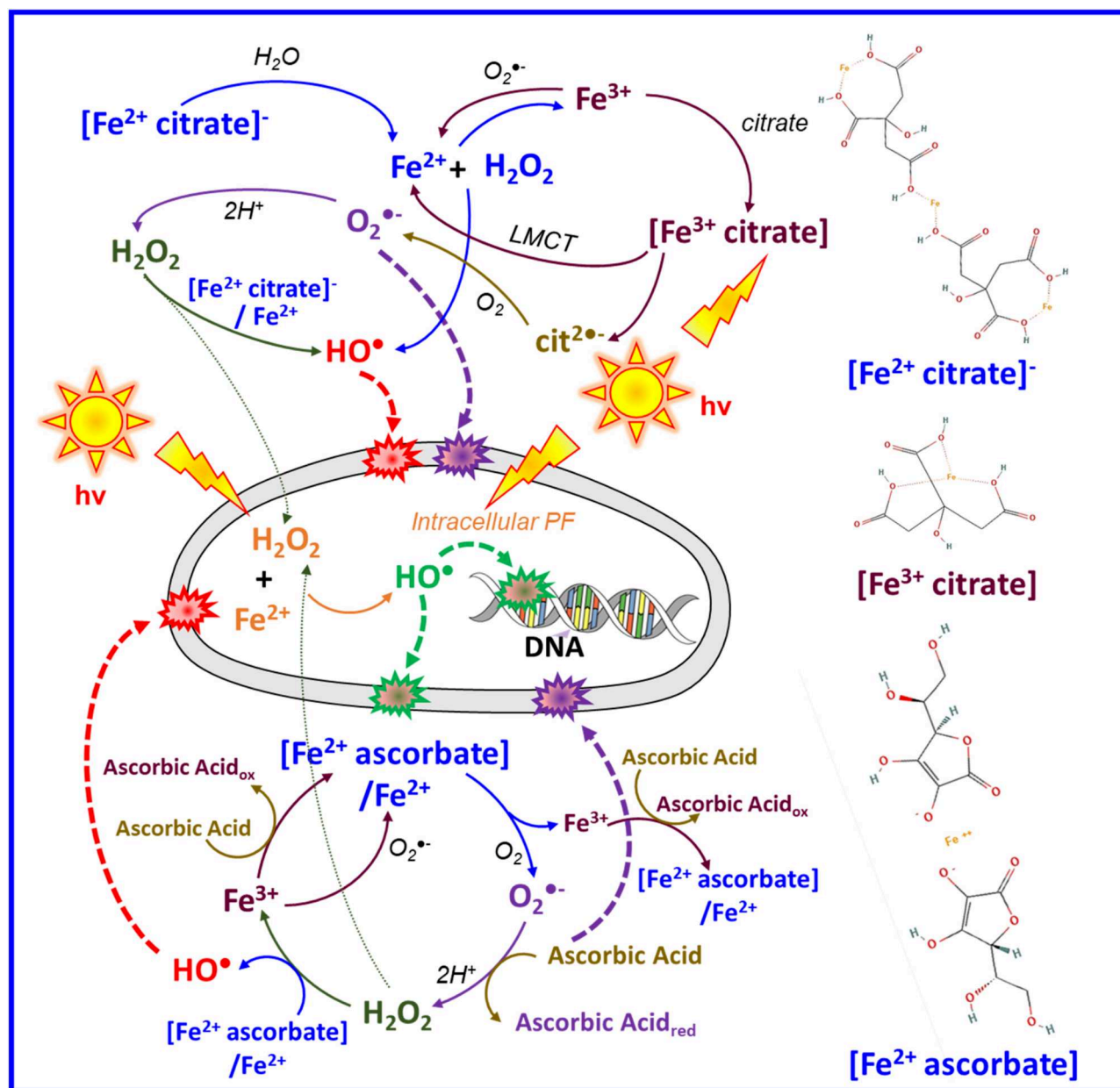
Fig. 4. Schematic of the bacterial inactivation pathways of the solar photo-Fenton process with complexed Fe (Fe:L), with emphasis on LMCT events. The figure is based on info from previous literature (Hou et al., 2016; Ruales-Lonfat et al., 2016).

and increase the efficiency of LMCT. The enhanced photo-Fenton process with AA in Fig. 5b shows the optimum balance between the above-mentioned factors owing to its ability to adequately stabilize iron at near neutral pH but with a low Kf' (see Fig. 3) and its highly stable radical form involved in the LMCT. Generalizing this phenomenon, the ligands' effect on the photo-Fenton process (Fig. 5d) follows, in its majority, the trends of Kf' in Fig. 3.

3.4. Bacterial inactivation with synthetic ligands

EDTA, EDDS, and NTA are well-known iron ligands that were tested for comparison with previously tested natural ligands. First, the toxicity of these acids to bacteria was tested (in the dark, with no iron). Figure S4 in the SI shows that the bacterial concentration is stable with all ligands; hence, they are not directly toxic to bacteria at the selected levels of experimental conditions.

Figs. 6a and 6b show the inactivation experiments with Fe(II) and Fe

(III), respectively, using EDTA, EDDS, and NTA as ligands, in the absence of H_2O_2. The results showed a detrimental effect of the synthetic ligands on bacterial inactivation in both cases. The slow inactivation kinetics are likely due to the behavior of the ligands as reactive species targets competing with bacterial inactivation. Specifically, EDTA has the highest starting TOC and the lowest inactivation activity, whereas for EDDS and NTA, the balance between Kf' and TOC reduction (see below in the text and Fig. 3) is in favor of the former because EDDS is more active. It is also noteworthy that the solar Fe-L enhanced process with synthetic ligands did not lead to a higher inactivation compared to that with organic acids. Hence, the baseline of the natural processes with acids is an enhancement itself.

Conversely, Figs. 6c and 6d show that the synthetic ligands have a beneficial effect on disinfection when tested in the presence of H_2O_2, which is corroborated by previous studies (De Luca et al., 2014; Šima and Makáňová, 1997). This behavior can be attributed to the high Kf' of iron at near-neutral pH, which is one of the necessary conditions for
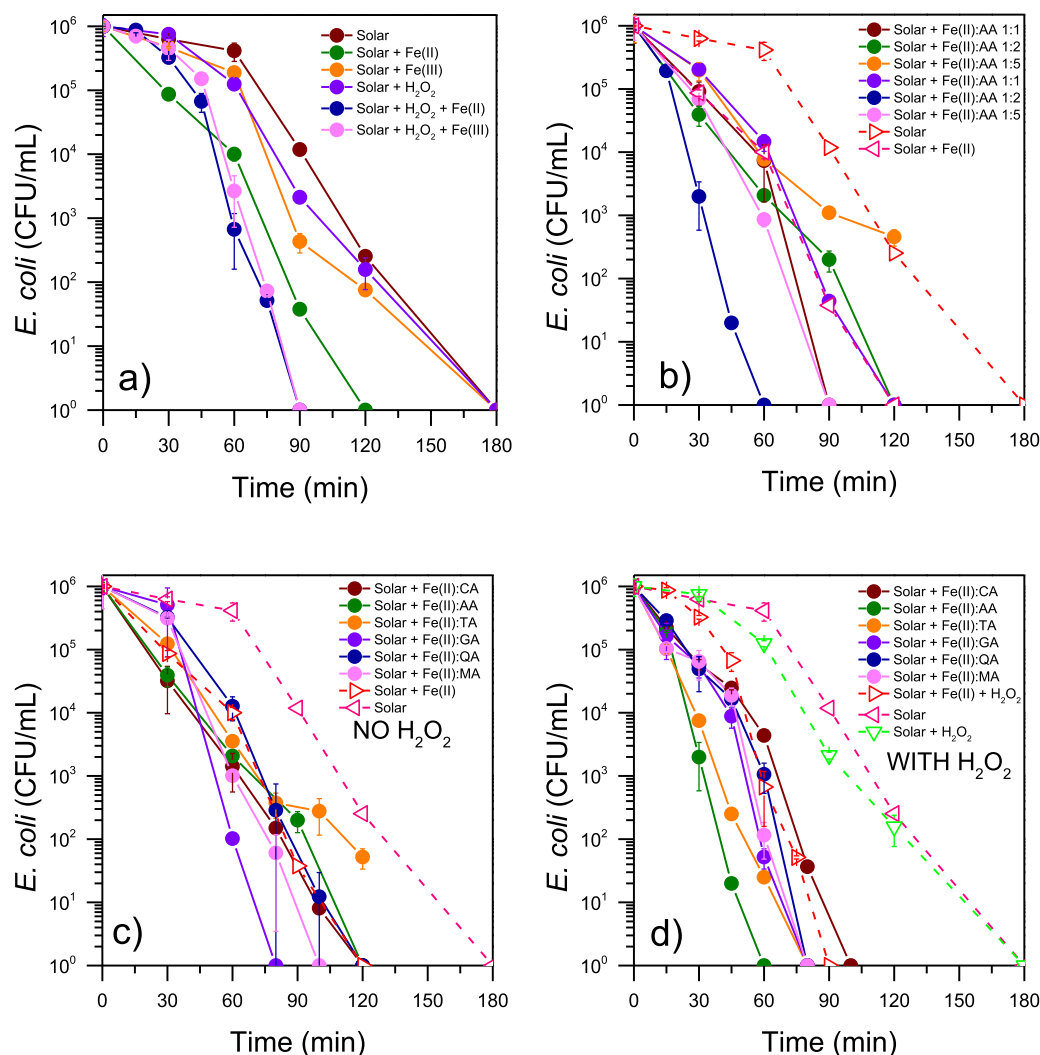
Fig. 5. a) Standard experiments for bacterial inactivation (solar light only, solar + H_2O_2, Solar + Fe^{2+}, Solar + Fe^{3+}, Solar + H_2O_2 + Fe^{2+}, and solar + H_2O_2 + Fe^3). The initial conditions were [$Fe^{2+,3+}$] = 1 mg/L, [H_2O_2] = 10 mg/L, and 900 W/m². b) Bacterial inactivation with iron(II)–ascorbic acid complexes at three different molar ratios (1:1, 1:2, and 1:5). Initial conditions: [Fe^{2+}] = 1 mg/L; [H_2O_2] = 10 mg/L; 900 W/m². Figures c) and d) represent bacterial inactivation with iron(II, III)-ligand complexes (molar ratio 1:2), where the ligands were citric, tartaric, ascorbic, malic, glutamic, and quinic acids. c) Solar + Fe + ligand; d) Solar+ Fe + ligand + H_2O_2. Initial conditions: [Fe^{2+}, Fe^{2+}] = 1 mg/L; [H_2O_2] = 10 mg/L; 900 W/m².

efficient LMCT. However, competition between the TOC of the ligand and disinfection efficiency could still be observed because the process with NTA, which had the lowest starting TOC (see Fig. 7), was the most efficient with both Fe(II) and Fe(III). These results further corroborate the higher influence on the process of the ligand and its amount compared to the influence of the central ion.

The highest efficiency of the process promoted by NTA is again corroborated by dissolved iron and consumption of H_2O_2 (see Figure S5b, c in the SI), which indicates a higher Fenton activity in that case. Interestingly, Figure S5b shows that the Fe(III)-NTA system maintained a constant amount of dissolved iron in all the treatments, suggesting that NTA can complex all the iron ions present in the bulk and release them by LMCT. However, in the presence of iron(II), the concentration of dissolved iron decreased at the beginning of the process. This is possibly due to the diffusion of Fe^{2+} ions through the cell. It is also interesting to note that with EDTA and EDDS, the TOC was only reduced by ~50 % compared with 70–90 % in the case of natural ligands. Indeed, organometallic complexes, such as those involved in this study, are generally less susceptible to oxidative reactions; hence, the equilibrium of the free ligand with its complexed form protects the former from drastic degradation due to the generated ROS. This occurs

because if the ligand is bound to a central metal, it will be less electronegative and, hence, less prone to attack by electrophilic ROS species. Indeed, EDTA and EDDS presented the highest Kf' at near-neutral pH, namely, the operative conditions of this investigation (see below in the text). Therefore, they can properly stabilize iron in solution, thus preserving the degradation of the ligand.

3.5. Fruit juice and peel infusion as additives to enhance bacterial inactivation: the "fruto-Fenton" process

Figs. 8a and b present the results with fruit juice or infusion, respectively, used instead of pure organic ligands to promote a natural organic ligand-assisted photo-Fenton bacterial inactivation ("*fruto-Fenton*"). In this study, lemons and oranges were used to obtain fruit juices and peel infusions. Fig. 8a shows a better inactivation of lemon juice than orange juice, and with both fruits, the inactivation was faster when Fe(II) was used instead of Fe(III), corroborating the previous results in this investigation. The high H_2O_2 consumption in both cases with lemon and orange juice confirms the high Fenton reaction activity (see Fig. 8c, d) in either bacterial inactivation or TOC reduction. Fig. 8c shows a higher presence of dissolved iron in lemon juice than in orange juice,
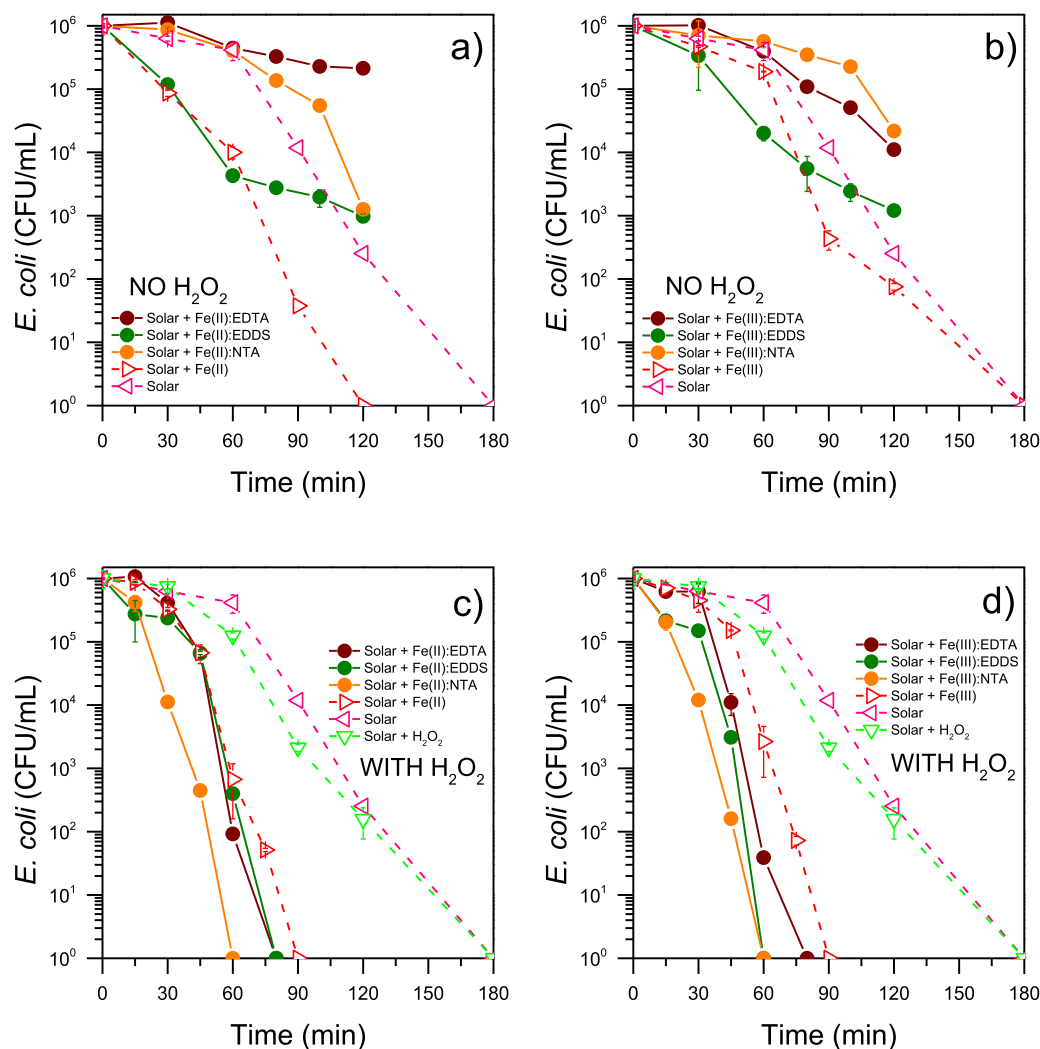
Fig. 6. Bacterial inactivation with iron and iron-synthetic acid complexes (molar ratio 1:2) for EDTA, EDDS, and NTA. A) Solar/Fe^{2+}-ligand; B) Solar/Fe^{3+}-ligand; C) Solar/Fe^{2+}-ligand/H_2O_2; D) Solar/Fe^{3+}-ligand/H_2O_2. The initial conditions were [$Fe^{2+,3+}$] = 1 mg/L, [H_2O_2] = 10 mg/L, and 900 W/m^2.
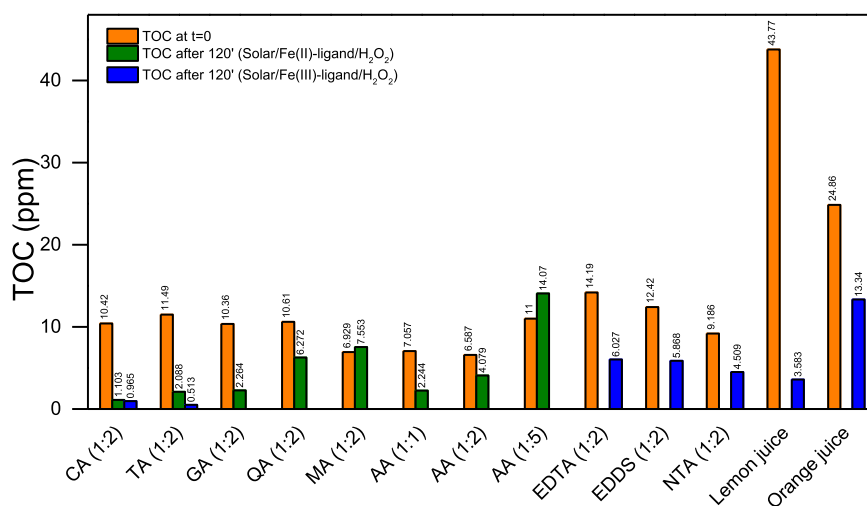

Fig. 7. Initial and final TOC during bacterial inactivation experiments with either Fe^{2+} or Fe^{3+} in the presence of a ligand and H_2O_2.

which likely explains the higher efficiency of the former compared to the latter (Moncayo-Lasso et al., 2012). This result also implies that lemon juice has the highest ability to keep iron ions in solution. In addition, in the case of fruit juice, the efficiency of inactivation is mostly related to the chelating agents (acids present in the juices) rather than to the oxidation state of the iron, as can be seen with the evolution of the total
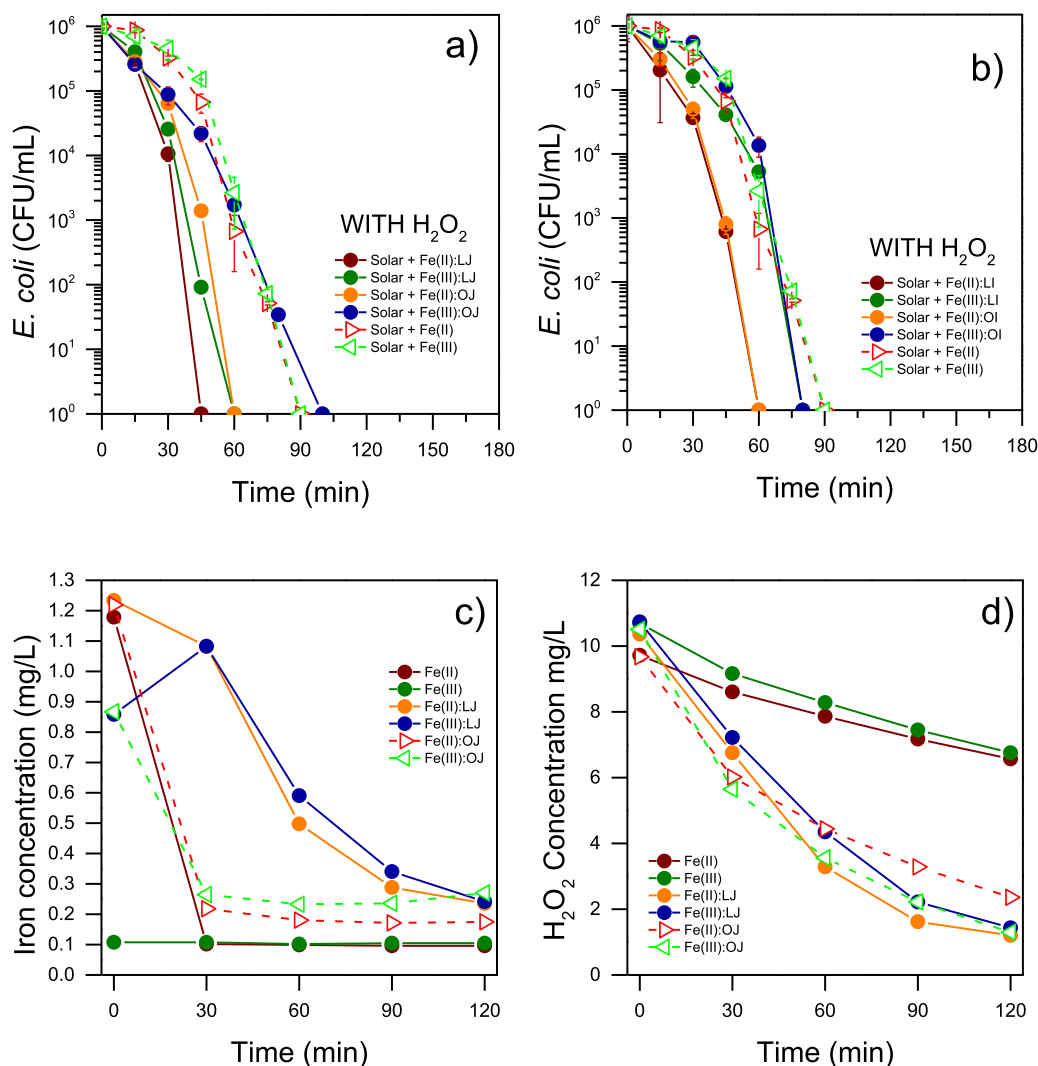
Fig. 8. a) Bacterial inactivation by the photo-Fenton process using lemon and orange juices (LJ and OJ, respectively). b) Bacterial inactivation by the photo-Fenton process with lemon and orange infusions. In both cases, the initial conditions were $[Fe^{2+}, Fe^{3+}] = 1$ mg/L, $[H_2O_2] = 10$ mg/L, and 900 W/m^2, while fruit juices and infusions were dosed, as mentioned in Table 1. Evolution of c) total dissolved iron, and d) H_2O_2 total dissolved iron concentrations in the photo-Fenton process for bacterial inactivation with iron-synthetic acid complexes (EDTA, EDDS, and NTA).

dissolved iron concentration (see Fig. 8c).

Fig. 8b shows the results of lemon and orange infusions from fruit peels. The advantage of this process is that it uses food waste instead of juice, which is a high-value product. In this case, the oxidation state of iron has a greater influence on inactivation than the chelating agents. With Fe(II), both lemon and orange infusions led to complete inactivation after 60 min, whereas with Fe(III), complete inactivation was achieved only after 80 min. In both cases, lemons were slightly more effective than oranges, in line with the experiments with the juices.

In addition to the initial TOC, Fig. 7 shows the final values, where a higher TOC decrease in experiments with lemon juice than orange juice during the reaction time was observed. As mentioned, even though TOC elimination is beneficial for drinking water requirements, it means that lemon juice competes more with bacterial disinfection. However, since the inactivation is more efficient with lemon than orange juice and there is a higher concentration of dissolved iron over time with the former, it follows that the mixture of chelating agents from lemon juice has a higher ability to stabilize iron in solution and lead to an efficient LMCT. The higher disinfection efficiency, along with the higher ability to stabilize iron, may also be due to the presence of other non-detectable organic agents such as flavonoids or tannic acids that play a role in LMCT (García-Ballesteros et al., 2016). These results demonstrated that

lemon juice can be effectively applied, leading to an efficient fruto-Fenton process.

3.6. Suitability of the proposed treatment for drinking water

Naturally, the question that arises in experiments using acids as enhancements, even if they are natural organic acids, is the evolution of the pH of the matrix. The pH can influence iron dissolution and, in turn, lead to a more efficient photo-Fenton application. For this purpose, the pH of the water was monitored throughout the process. Fig. 9 shows that the pH did not change significantly during inactivation. Any ligand addition in Milli-Q water leads to a starting pH between 4.5 and 5, except for EDTA and EDDS, which lead to a pH of approximately 7. These values can partially explain the activity, considering that Milli-Q water has a starting pH <6; hence, the reduction was within the acidic range. We do note, however, that Milli-Q water has virtually no buffer capacity and may be subject to higher pH variations than natural waters.

In addition, according to the World Health Organization, a health-based guideline value for pH is not necessary, although values as low as 4 are recommended (World Health Organization, 2007). This recommendation is to be considered as orientative; lemon and orange juices are weak acids and their consumption does not require control,
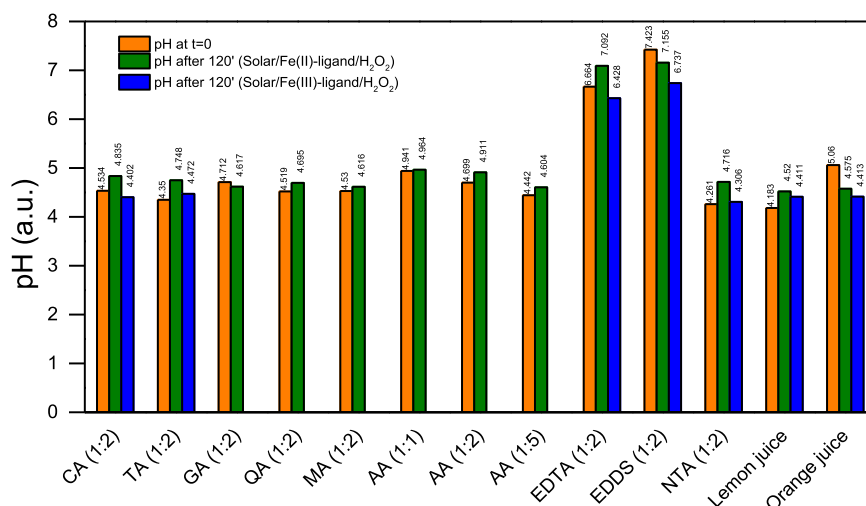
Fig. 9. Initial and final pH during bacterial inactivation experiments with either Fe^{2+} or Fe^{3+} in the presence of a ligand and H_2O_2. Please note that the pH is rather constant over the process, with a variation of less than one unit.

even if the pH of lemon juice itself is 2.4 (World Health Organisation, 2007), or, for example, the pH of a very well-known brand of dark-colored fizzy refreshment is around 2.5. The final pH values of the inactivation systems without ligands (solar/Fe(II)/H_2O_2 and solar/Fe (III)/H_2O_2) were 4.85 and 4.50, respectively. The pH range reached during these experiments is acceptable for drinking water.

Besides the pH, the addition of acids increases the TOC, which is an undesirable component in drinking water, while acting as a target for ROS and hindering bacterial inactivation. To this end, the TOC was monitored during the bacterial inactivation experiments (Fig. 7a). In all cases, TOC was clearly reduced; however, its reduction has a controversial effect. The TOC reduction is beneficial because a decrease in the organic matter concentration is a requirement, for instance, in drinking water treatment. However, the observed reduction in DOM further confirmed the competition between ligands and bacteria, which eventually led to a decrease in inactivation efficiency. Here, in the less active cases, namely CA, AA, TA, and GA, $a \approx 90$ % TOC reduction was observed, thus a higher competition of the ligand against bacterial inactivation. Conversely, with GA and MA, the TOC reduction was less than 70 %, and inactivation was faster. Even though the same competition is involved when the complexes facilitate disinfection in the presence of H_2O_2, this effect is apparently mitigated because the balance

favors bacterial inactivation in most cases (see Fig. 5b), which is therefore likely due to an LMCT mechanism.

Figs. 10a and 10b corroborate the faster photo-Fenton inactivation in the presence of AA, with higher H_2O_2 consumption and higher residual dissolved iron. This corresponds to effective Fenton reaction activity and faster bacterial inactivation. In general, a correlation between the higher consumption of H_2O_2 and higher residual dissolved iron was found for all ligands. This indicates that these acids avoid the precipitation of iron, thus leading to more Fe^{2+} available for the Fenton reaction and a higher H_2O_2 consumption through this process, even if the ligand is also a target. However, the trend is less clear when observing bacterial inactivation itself because the phenomena involved are multiple and not easy to correlate with H_2O_2/iron consumption.

Finally, it is worth taking into account the potential of bacterial regrowth. The presence of readily biodegradable organic acids constitutes an excellent source of carbon for bacterial metabolism, in contrast to natural organic matter, for example, in a river, which is predominantly not so easily biodegradable, and/or a residual of physicochemical and biogenic processes. In our assay, we kept the samples with CA and AA in the dark for 24 h after treatment to assess risk, but no regrowth was observed. However, given that this was assessed only in two acids, Milli-Q water, and only for 24 h, the outcome is not definitive, and a
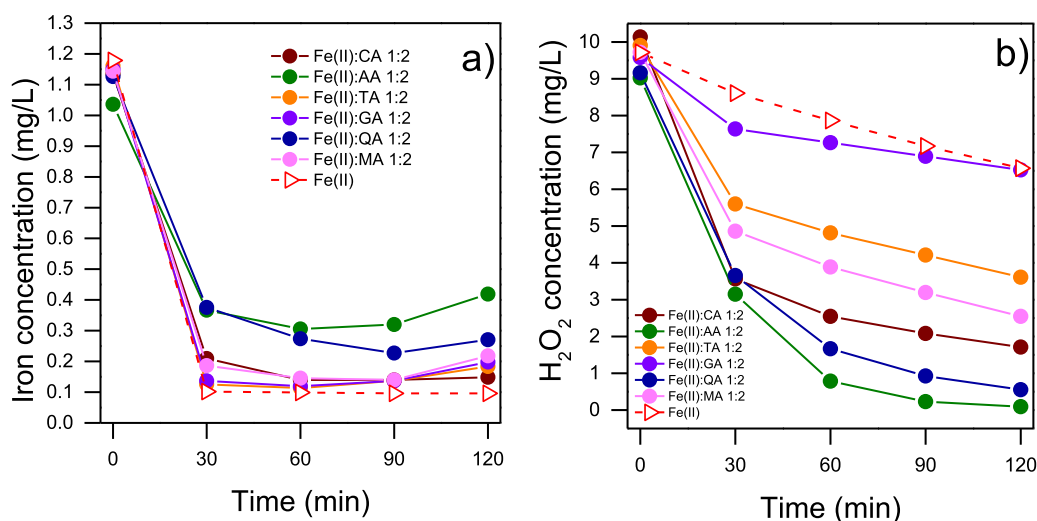

Fig. 10. Evolution of a) total dissolved iron concentrations and b) H_2O_2 in the photo-Fenton process for bacterial inactivation with iron(II)-ligands.

larger-scale study would be called for, especially if long-term storage of water is envisioned.

As a provisional conclusion, we suggest that the fruit ligand-containing version of the photo-Fenton process has notably high performance without compromising water in terms of TOC and pH. However, given the fact that the experiments were performed in Milli-Q water and, consequently, without the buffer effect and lower pH, and in UVB-transparent glass reactors under stirring, it might be beneficial to assess the feasibility and performance of the process in natural water treatment.

3.7. Ligand-mediated photo-Fenton disinfection in lake leman water

Figs. 11a and 11b show the results of SODIS and fruto-Fenton-assisted SODIS in the water of Leman Lake, in 500-mL PET bottles without agitation. The results show that the matrix has a detrimental effect on the SODIS and photo-Fenton processes, compared with the results shown in Fig. 5. The higher natural pH of the matrix (8.3–8.5 vs. <6 in MQ), along with the presence of numerous organic elements, could reasonably affect the performance of a pH-dependent radical process, and these results have to be taken as a benchmark for the matrix. Indeed, by lowering the pH, the efficiency increased with an optimum pH of 6 (see Fig. 11b). This U-shape trend of disinfection efficiency compared to the pH in the lake water is likely due to the presence of NOM, which can act both as an iron ligand or a strong radical scavenger depending on the interaction with the central metal, and hence on the pH.

Figure S6 in the SI shows that the *ex situ* addition of the iron:ligand complexes (specifically with CA and AA) does not exert a significant beneficial effect on disinfection. In addition, the higher the increase in the amount of ligand (ranging from 1:2 to 1:10), the lower the disinfection efficiency. Hence, the matrix effect strongly affects the actual application of the fruto-Fenton process. Therefore, the strategy for a potentially "real," field application of this process had to be adapted.

Fig. 12 shows an assessment of different iron:CA and iron:H_2O_2 ratios, along with the *in situ* and *ex situ* complex preparation. Fig. 12a shows that the in-situ preparation of the complex has a beneficial effect on the efficiency of disinfection compared to the normal PF process. It also shows that an iron:CA ratio of 1:1 is the optimum value. Fig. 12b shows the effect of double the amount of iron (2 ppm compared to 1 ppm previously used), whose results were overall beneficial.

In summary, Fig. 12 shows that an *in situ* preparation of the complex can speed up the inactivation rates, and by doubling the amount of iron,

the process is further enhanced because a lower amount of ligand is needed to enhance bacterial inactivation. These results pave the way for effective application of the fruto-Fenton process under field conditions.

4. Conclusions

This study provides a holistic interpretation and correlation of the ligands' molecular structures and thermodynamic properties (Kf') with their efficacy in bacterial disinfection. The possibility of applying the treatment even at alkaline pH in natural surface waters and the use of low-cost, easy-to-use, and sustainable elements, such as fruit extracts, satisfies the acceptance criteria for resource-poor communities and holds potential for further field implementation.

The conclusions drawn from this study are as follows:

- The less efficient variations in the ligand-mediated processes in the absence of H_2O_2 were those with synthetic acids (EDTA, EDDS, and NTA), regardless of whether Fe(II) or Fe(III) was used. For the photo-Fenton processes with Fe(II), all ligands promoted complete inactivation between 60 and 80 min, except for citric acid (100 min) and lemon juice (45 min). This indicates that natural organic acids are as effective as synthetic acids, which are well known to enhance the photo-Fenton process. More importantly, the efficacy of the fruit extracts is in the same order of magnitude, which constitutes a great find with a view to a possi application.
- From Table 2 we can state that the higher the Kf' is, less efficient the photo-Fenton process with Fe(II) will be, from a general standpoint. However, multiple factors must be considered and correlated with a more rigorous case-by-case interpretation of the results. For instance, the starting TOC by the ligand can be a target for reactive species competing with bacterial disinfection, but at the same time, is a necessary evil. An optimum amount of ligand that may keep iron in solution at near neutral pH and allow efficient LMCT has to be selected; this study defined 1:2 as the optimum Fe:L ratio. Furthermore, the higher the photoactivity of the ligand, the higher its ability to stabilize the radical species in its molecular structure, leading to an efficient LMCT.

Balancing all the abovementioned factors and the viability of the ligands, this investigation concludes that AA is the best pure ligand for enhancing photo-Fenton inactivation. Nevertheless, fruit extracts resulted in an effective 6-logU decrease in *E. coli*, which is very encouraging from the perspective of efficient solar bacterial inactivation
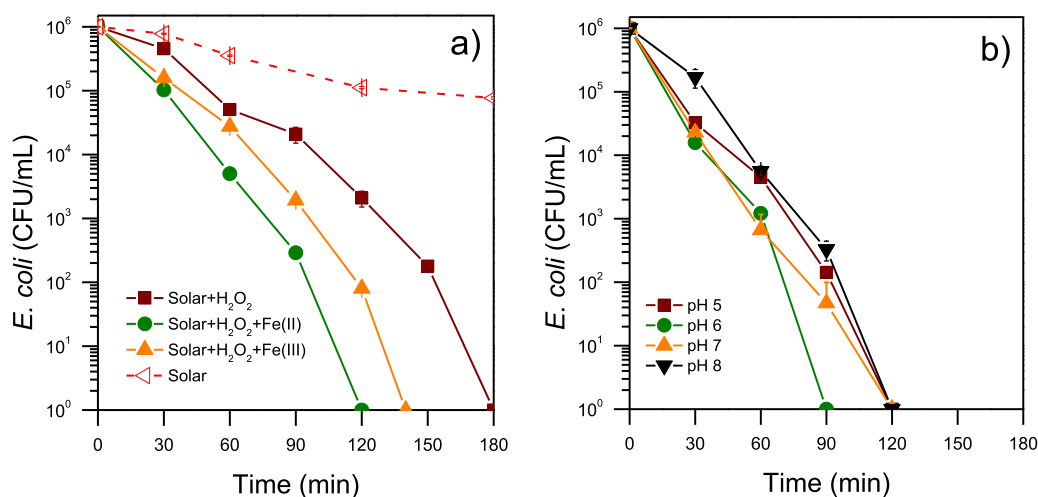

Fig. 11. a) Effect of photo-Fenton and its constituents on disinfection of Leman Lake water. The pH drops 0.3 units after the addition of Fe(II) (from 8 to 7.7) and 0.2 units after the addition of Fe(III) (from 8.3 to 8.1). b) Effect of pH on the efficiency of the photo-Fenton process with Fe(II) for water disinfection. After the addition of Fe(II), the pH changed from 5 to 5.2, from 6 to 6.6, from 7.1 to 7.3, and from 8 to 7.
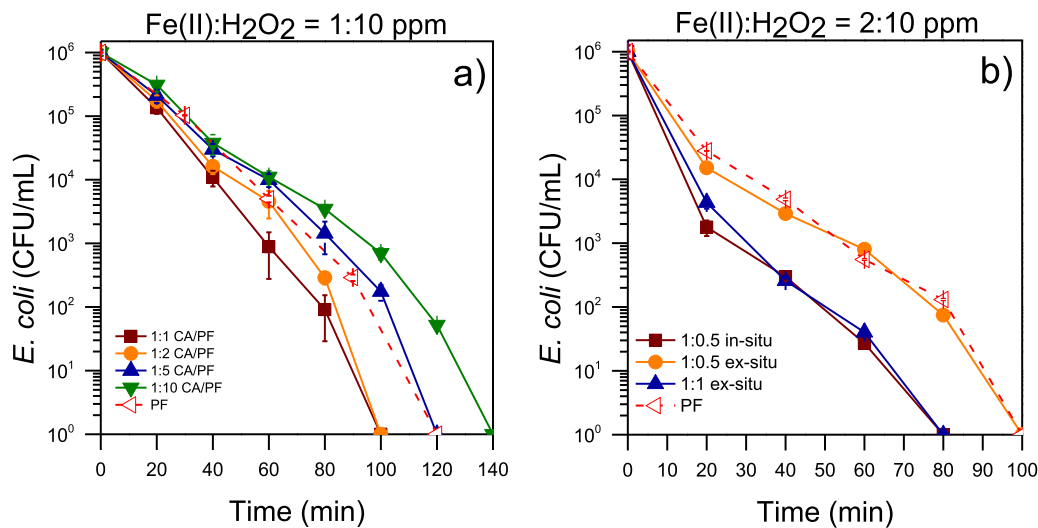
Fig. 12. a) Effect of iron:CA ratio after in-situ preparation during a PF/Fe(II) process using 1 and 10 ppm of iron and H$_2$O$_2$, respectively. The pH conditions before and after the addition of iron were stable at near-neutral pH. b) Effect of the increase in the iron amount on the iron:CA ratio and disinfection efficiency. The amounts of iron and H$_2$O$_2$ were 2 ppm and 10 ppm, respectively. The pH conditions before and after the addition of iron were stable at near-neutral pH.

Table 2

Summary of the most relevant results of the bacterial inactivation time (min) under the different conditions tested and compared with Kf' at pH 7 for each iron-ligand complex. The iron-acid ratio was 1:2 for each ligand. The table presents the most promising results in red, while the reference inactivation time without ligands is bolded.

Only solar light	180 min				
Solar + H$_2$O$_2$	180 min				
Ligand	Kf' (pH 7)	Fe(II)	Fe(II)+ H$_2$O$_2$	Fe(III)	Fe(III)+ H$_2$O$_2$
–		**120 min**	**90 min**	**180 min**	**90 min**
Citric acid	6.0E3	120 min	100 min	120 min	100 min
Malic acid	4.0E2	100 min	80 min		
Quinic acid	2.8E2	120 min	80 min		
Tartaric acid	1.7E2	>120 min	80 min	100 min	100 min
Ascorbic acid	7.2E-5	120 min	60 min		
Glutamic acid	–	80 min	80 min		
EDTA	5.3E11	>120 min	80 min	>120 min	80 min
EDDS	5.9E6	>120 min	80 min	>120 min	60 min
NTA	2.7E6	>120 min	60 min	>120 min	60 min
Lemon juice			45 min		60 min
Orange juice			60 min		100 min
Lemon infusion			60 min		80 min
Orange infusion			60 min		80 min

with natural and biodegradable products in challenging contexts. In addition, fruit extracts are the most viable elements to be employed in this enhanced, fruto-Fenton bacterial inactivation process, since fruit juice is easy to access and peel infusions allow the recycling of waste material. Specifically, the photo-Fenton process with lemon juice showed fast bacterial inactivation (45 min), high H$_2$O$_2$ consumption, a good ability to chelate iron (thus avoiding its precipitation), and a important TOC decrease in TOC. Therefore, ideal conditions for efficient disinfection are met.

CRediT authorship contribution statement

Giulio Farinelli: Data curation, Formal analysis, Investigation,

Methodology, Writing – original draft. **Stefanos Giannakis:** Conceptualization, Funding acquisition, Methodology, Project administration, Resources, Supervision, Validation, Visualization, Writing – review & editing. **Aline Schaub:** Data curation, Formal analysis, Methodology. **Mona Kohantorabi:** Data curation, Formal analysis, Methodology, Writing – review & editing. **Cesar Pulgarin:** Conceptualization, Data curation, Funding acquisition, Methodology, Project administration, Resources, Supervision, Validation, Visualization, Writing – review & editing.

Declaration of competing interest

The authors declare no financial/personal relationships which may be considered as potential competing interests.

Data availability

Data will be made available on request.

Supplementary materials

Supplementary material associated with this article can be found, in the online version, at doi:10.1016/j.watres.2024.121518.

References

Abida, O., Mailhot, G., Litter, M., Bolte, M., 2006. Impact of iron-complex (Fe(iii)–NTA) on photoinduced degradation of 4-chlorophenol in aqueous solution. Photochem. Photobiol. Sci. 5, 395–402. https://doi.org/10.1039/b518211e.

Abrahamson, H.B., Rezvani, A.B., Brushmiller, J.G., 1994. Photochemical and spectroscopic studies of complexes, of iron(III) with citric acid and other carboxylic acids. Inorganica Chim. Acta 226, 117–127. https://doi.org/10.1016/0020-1693(94)04077-X.

Ahile, U.J., Wuana, R.A., Itodo, A.U., Sha'Ato, R., Dantas, R.F., 2020. Stability of iron chelates during photo-Fenton process: the role of pH, hydroxyl radical attack and temperature. J. Water Process Eng. 36, 101320 https://doi.org/10.1016/j.jwpe.2020.101320.

Ahile, U.J., Wuana, R.A., Itodo, A.U., Sha'Ato, R., Malvestiti, J.A., Dantas, R.F., 2021. Are iron chelates suitable to perform photo-Fenton at neutral pH for secondary effluent treatment? J. Environ. Manage. 278, 111566 https://doi.org/10.1016/j.jenvman.2020.111566.

Attar, S.B.-E., Soriano-Molina, P., Pichel, N., París-Reche, A., Plaza-Bolaños, P., Agüera, A., Pérez, J.A.S., 2023. Continuous flow operation of solar photo-Fenton fused with NaOCl as a novel tertiary treatment. J. Hazard. Mater. 460, 132354 https://doi.org/10.1016/j.jhazmat.2023.132354.

Braun, V., 2001. Iron uptake mechanisms and their regulation in pathogenic bacteria. Int. J. Med. Microbiol. 291, 67–79.

Cabiscol, E., Tamarit, J., Ros, J., 2000. Oxidative stress in bacteria and protein damage by reactive oxygen species. Int. Microbiol. 3, 3–8.

Chaúque, B.J.M., Rott, M.B., 2021. Solar disinfection (SODIS) technologies as alternative for large-scale public drinking water supply: advances and challenges. Chemosphere 281, 130754. https://doi.org/10.1016/j.chemosphere.2021.130754.

Cieśla, P., Kocot, P., Mytych, P., Stasicka, Z., 2004. Homogeneous photocatalysis by transition metal complexes in the environment. J. Mol. Catal. A Chem. 224, 17–33. https://doi.org/10.1016/j.molcata.2004.08.043.

Clarizia, L., Russo, D., Di Somma, I., Marotta, R., Andreozzi, R., 2017. Homogeneous photo-Fenton processes at near neutral pH: a review. Appl. Catal. B Environ. 209, 358–371. https://doi.org/10.1016/j.apcatb.2017.03.011.

CLARK, A., PRENZLER, P., SCOLLARY, G., 2007. Impact of the condition of storage of tartaric acid solutions on the production and stability of glyoxylic acid. Food Chem 102, 905–916. https://doi.org/10.1016/j.foodchem.2006.06.029.

Coha, M., Farinelli, G., Tiraferri, A., Minella, M., Vione, D., 2021. Advanced oxidation processes in the removal of organic substances from produced water: potential, configurations, and research needs. Chem. Eng. J. 414, 128668 https://doi.org/10.1016/j.cej.2021.128668.

Daoudy, M., Sowers, J., Weinthal, E., 2022. What is climate security? Framing risks around water, food, and migration in the Middle East and North Africa. WIREs Water 9, e1582. https://doi.org/10.1002/wat2.1582.

De Luca, A., Dantas, R.F., Esplugas, S., 2014. Assessment of iron chelates efficiency for photo-Fenton at neutral pH. Water Res 61, 232–242. https://doi.org/10.1016/j.watres.2014.05.033.

Farinelli, G., Minella, M., Pazzi, M., Giannakis, S., Pulgarin, C., Vione, D., Tiraferri, A., 2020. Natural iron ligands promote a metal-based oxidation mechanism for the Fenton reaction in water environments. J. Hazard. Mater. 393, 122413 https://doi.org/10.1016/j.jhazmat.2020.122413.

Fernandes, A., Makoś, P., Wang, Z., Boczkaj, G., 2020. Synergistic effect of TiO2 photocatalytic advanced oxidation processes in the treatment of refinery effluents. Chem. Eng. J. 391, 123488 https://doi.org/10.1016/j.cej.2019.123488.

Fiorentino, A., Cucciniello, R., Di Cesare, A., Fontaneto, D., Prete, P., Rizzo, L., Corno, G., Proto, A., 2018. Disinfection of urban wastewater by a new photo-Fenton like process using Cu-iminodisuccinic acid complex as catalyst at neutral pH. Water Res 146, 206–215. https://doi.org/10.1016/j.watres.2018.08.024.

Flores, P., Hellín, P., Fenoll, J., 2012. Determination of organic acids in fruits and vegetables by liquid chromatography with tandem-mass spectrometry. Food Chem 132, 1049–1054. https://doi.org/10.1016/j.foodchem.2011.10.064.

García-Ballesteros, S., Mora, M., Vicente, R., Sabater, C., Castillo, M.A., Arques, A., Amat, A.M., 2016. Gaining further insight into photo-Fenton treatment of phenolic compounds commonly found in food processing industry. Chem. Eng. J. 288, 126–136. https://doi.org/10.1016/j.cej.2015.11.031.

García-Gil, Á., García-Muñoz, R.A., McGuigan, K.G., Marugán, J., 2021. Solar water disinfection to produce safe drinking water: a review of parameters, enhancements, and modelling approaches to make SODIS faster and safer. Molecules 26, 3431. https://doi.org/10.3390/molecules26113431.

García-Gil, Á., Pablos, C., García-Muñoz, R.A., McGuigan, K.G., Marugán, J., 2020. Material selection and prediction of solar irradiance in plastic devices for application of solar water disinfection (SODIS) to inactivate viruses, bacteria and protozoa. Sci. Total Environ. 730, 139126 https://doi.org/10.1016/j.scitotenv.2020.139126.

Giannakis, S., Gupta, A., Pulgarin, C., Imlay, J., 2022. Identifying the mediators of intracellular E. coli inactivation under UVA light: the (photo) Fenton process and singlet oxygen. Water Res 221, 118740. https://doi.org/10.1016/j.watres.2022.118740.

Giannakis, S., Polo López, M.I., Spuhler, D., Sánchez Pérez, J.A., Fernández Ibáñez, P., Pulgarin, C., 2016. Solar disinfection is an augmentable, in situ -generated photo-Fenton reaction—Part 1: a review of the mechanisms and the fundamental aspects of the process. Appl. Catal. B Environ. 199, 199–223. https://doi.org/10.1016/j.apcatb.2016.06.009.

Gomes Júnior, O., Silva, V.M., Machado, A.E.H., Sirtori, C., Lemos, C.R., Freitas, A.M., Trovó, A.G., 2018. Correlation between pH and molar iron/ligand ratio during ciprofloxacin degradation by photo-Fenton process: identification of the main transformation products. J. Environ. Manage. 213, 20–26. https://doi.org/10.1016/j.jenvman.2018.02.041.

Gualda-Alonso, E., Soriano-Molina, P., Casas López, J.L., García Sánchez, J.L., Plaza-Bolaños, P., Agüera, A., Sánchez Pérez, J.A., 2022. Large-scale raceway pond reactor for CEC removal from municipal WWTP effluents by solar photo-Fenton. Appl. Catal. B Environ. 319, 121908 https://doi.org/10.1016/j.apcatb.2022.121908.

Guilhermino, L., Diamantino, T.C., Ribeiro, R., Gonçalves, F., Soares, A.M.V.M., 1997. Suitability of test media containing EDTA for the evaluation of acute metal toxicity todaphnia magnastraus. Ecotoxicol. Environ. Saf. 38, 292–295. https://doi.org/10.1006/eesa.1997.1599.

Halliwell, B., Aruoma, O.I., 1991. DNA damage by oxygen-derived species Its mechanism and measurement in mammalian systems. FEBS Lett 281, 9–19.

Hou, X., Shen, W., Huang, X., Ai, Z., Zhang, L., 2016. Ascorbic acid enhanced activation of oxygen by ferrous iron: a case of aerobic degradation of rhodamine B. J. Hazard. Mater. 308, 67–74. https://doi.org/10.1016/j.jhazmat.2016.01.031.

Kocot, P., Karocki, A., Stasicka, Z., 2006. Photochemistry of the Fe(III)–EDTA complexes. J. Photochem. Photobiol. A Chem. 179, 176–183. https://doi.org/10.1016/j.jphotochem.2005.08.016.

Koppenol, W.H., 2001. The Haber-Weiss cycle –70 years later. Redox Rep 6, 229–234. https://doi.org/10.1179/135100001101536373.

Li, J., Mailhot, G., Wu, F., Deng, N., 2010. Photochemical efficiency of Fe(III)-EDDS complex: OH radical production and 17β-estradiol degradation. J. Photochem. Photobiol. A Chem. 212, 1–7. https://doi.org/10.1016/j.jphotochem.2010.03.001.

Lloyd, D.R., Phillips, D.H., Carmichael, P.L., 1997. Generation of putative intrastand cross-links and strand breaks in DNA by transition metal ion-mediated oxygen radical attack. Chem. Res. Toxicol. 10, 393–400. https://doi.org/10.1021/tx960158q.

Manrique-Losada, L., Santanilla-Calderón, H.L., Serna-Galvis, E.A., Torres-Palma, R.A., 2022. Improvement of solar photo-Fenton by extracts of amazonian fruits for the degradation of pharmaceuticals in municipal wastewater. Environ. Sci. Pollut. Res. 29, 42146–42156. https://doi.org/10.1007/s11356-021-15377-1.

Mazhar, M.A., Khan, N.A., Ahmed, S., Khan, A.H., Hussain, A., Rahisuddin, Changani, F., Yousefi, M., Ahmadi, S., Vambol, V., 2020. Chlorination disinfection by-products in municipal drinking water – A review. J. Clean. Prod. 273, 123159 https://doi.org/10.1016/j.jclepro.2020.123159.

McGuigan, K.G., Conroy, R.M., Mosler, H.J., Preez, M.du, Ubomba-Jaswa, E., Fernandez-Ibañez, P., 2012. Solar water disinfection (SODIS): a review from bench-top to rooftop. J. Hazard. Mater. 235–236, 29–46. https://doi.org/10.1016/j.jhazmat.2012.07.053.

Mey, A.R., Gómez-Garzón, C., Payne, S.M., 2021. Iron Transport and Metabolism in Escherichia, Shigella, and Salmonella. Ecosal Plus 9, eESP00342020. https://doi.org/10.1128/ecosalplus.ESP-0034-2020.

Mitchell, S.M., Ullman, J.L., Teel, A.L., Watts, R.J., 2014. PH and temperature effects on the hydrolysis of three β-lactam antibiotics: ampicillin, cefalotin and cefoxitin. Sci. Total Environ. 466–467, 547–555. https://doi.org/10.1016/j.scitotenv.2013.06.027.

Moncayo-Lasso, A., Mora-Arismendi, L.E., Rengifo-Herrera, J.A., Sanabria, J., Benítez, N., Pulgarin, C., 2012. The detrimental influence of bacteria (E. coli, Shigella and Salmonella) on the degradation of organic compounds (and vice versa) in TiO2 photocatalysis and near-neutral photo-Fenton processes under simulated solar light. Photochem. Photobiol. Sci. 11, 821–827. https://doi.org/10.1039/c2pp05290c.

Nahman, A., de Lange, W., 2013. Costs of food waste along the value chain: evidence from South Africa. Waste Manag 33, 2493–2500. https://doi.org/10.1016/j.wasman.2013.07.012.

Oller, I., Malato, S., Sánchez-Pérez, J.A., 2011. Combination of advanced oxidation processes and biological treatments for wastewater decontamination—A review. Sci. Total Environ. 409, 4141–4166. https://doi.org/10.1016/j.scitotenv.2010.08.061.

Ozores Diez, P., Giannakis, S., Rodríguez-Chueca, J., Wang, D., Quilty, B., Devery, R., McGuigan, K., Pulgarin, C., 2020. Enhancing solar disinfection (SODIS) with the photo-Fenton or the Fe2+/peroxymonosulfate-activation process in large-scale plastic bottles leads to toxicologically safe drinking water. Water Res 186, 116387. https://doi.org/10.1016/j.watres.2020.116387.

Pan, G.H., Barras, A., Boussekey, L., Qu, X., Boukherroub, R., 2013. Photochemical reaction of vitamin C with silicon nanocrystals: polymerization, hydrolysis and photoluminescence. J. Mater. Chem. C 1, 5856. https://doi.org/10.1039/c3tc31082e.

Papoutsakis, S., Brites-Nóbrega, F.F., Pulgarin, C., Malato, S., 2015. Benefits and limitations of using Fe(III)-EDDS for the treatment of highly contaminated water at near-neutral pH. J. Photochem. Photobiol. A Chem. 303–304, 1–7. https://doi.org/10.1016/j.jphotochem.2015.01.013.

Pichel, N., Belachqer-El Attar, S., Soriano-Molina, P., Sánchez Pérez, J.A., 2023. Demonstrating the feasibility of a novel solar photo-Fenton strategy for full-scale operationalization according to EU 2020/741 disinfection targets for water reuse. Chem. Eng. J. 472, 144935 https://doi.org/10.1016/j.cej.2023.144935.

Polo-López, M.I., Sánchez Pérez, J.A., 2021. Perspectives of the solar photo-Fenton process against the spreading of pathogens, antibiotic-resistant bacteria and genes in the environment. Curr. Opin. Green Sustain. Chem. 27, 100416 https://doi.org/10.1016/j.cogsc.2020.100416.

Pulgarin, A., Decker, J., Chen, J., Giannakis, S., Ludwig, C., Refardt, D., Pick, H., 2022. Effective removal of the rotifer Brachionus calyciflorus from a Chlorella vulgaris microalgal culture by homogeneous solar photo-Fenton at neutral pH. Water Res 226, 119301. https://doi.org/10.1016/j.watres.2022.119301.

Pulgarin, A., Giannakis, S., Pulgarin, C., Ludwig, C., Refardt, D., 2020. A novel proposition for a citrate-modified photo-Fenton process against bacterial

contamination of microalgae cultures. Appl. Catal. B Environ. 265, 118615 https://doi.org/10.1016/j.apcatb.2020.118615.

Roca, M., Villegas, L., Kortabitarte, M.L., Althaus, R.L., Molina, M.P., 2011. Effect of heat treatments on stability of β-lactams in milk. J. Dairy Sci. 94, 1155–1164. https://doi.org/10.3168/jds.2010-3599.

Roccaro, P., Vagliasindi, F.G.A., Korshin, G.V., 2009. Changes in NOM fluorescence caused by chlorination and their associations with disinfection by-products formation. Environ. Sci. Technol. 43, 724–729. https://doi.org/10.1021/es801939f.

Ruales-Lonfat, C., Barona, J.F., Sienkiewicz, A., Bensimon, M., Vélez-Colmenares, J., Benítez, N., Pulgarín, C., 2015. Iron oxides semiconductors are efficients for solar water disinfection: a comparison with photo-Fenton processes at neutral pH. Appl. Catal. B Environ. 166–167, 497–508. https://doi.org/10.1016/j.apcatb.2014.12.007.

Ruales-Lonfat, C., Barona, J.F., Sienkiewicz, A., Vélez, J., Benítez, L.N., Pulgarín, C., 2016. Bacterial inactivation with iron citrate complex: a new source of dissolved iron in solar photo-Fenton process at near-neutral and alkaline pH. Appl. Catal. B Environ. 180, 379–390. https://doi.org/10.1016/j.apcatb.2015.06.030.

Samoili, S., Farinelli, G., Moreno-SanSegundo, J.Á., McGuigan, K.G., Marugán, J., Pulgarín, C., Giannakis, S., 2022. Predicting the bactericidal efficacy of solar disinfection (SODIS): from kinetic modeling of in vitro tests towards the in silico forecast of E. coli inactivation. Chem. Eng. J. 427, 130866 https://doi.org/10.1016/j.cej.2021.130866.

Scherer, R., Rybka, A.C.P., Ballus, C.A., Meinhart, A.D., Filho, J.T., Godoy, H.T., 2012. Validation of a HPLC method for simultaneous determination of main organic acids in fruits and juices. Food Chem 135, 150–154. https://doi.org/10.1016/j.foodchem.2012.03.111.

Seraghni, N., Belattar, S., Mameri, Y., Debbache, N., Sehili, T., 2012. Fe(III)-citrate-complex-induced photooxidation of 3-methylphenol in aqueous solution. Int. J. Photoenergy 2012, 1–10. https://doi.org/10.1155/2012/630425.

Šima, J., Makáňová, J., 1997. Photochemistry of iron (III) complexes. Coord. Chem. Rev. 160, 161–189. https://doi.org/10.1016/S0010-8545(96)01321-5.

Sinha, R.P., Häder, D.P., 2002. UV-induced DNA damage and repair: a review. Photochem. Photobiol. Sci. 1, 225–236. https://doi.org/10.1039/b201230h.

Spuhler, D., Andrés Rengifo-Herrera, J., Pulgarin, C., 2010. The effect of Fe2+, Fe3+, H2O2 and the photo-Fenton reagent at near neutral pH on the solar disinfection (SODIS) at low temperatures of water containing Escherichia coli K12. Appl. Catal. B Environ. 96, 126–141. https://doi.org/10.1016/j.apcatb.2010.02.010.

Sun New Haven, C.T.), Y. (The C.A.E.S., Pignatello, J.J., n.d. Chemical treatment of pesticide wastes. Evaluation of Fe(III) chelates for catalytic hydrogen peroxide oxidation of 2,4-D at circumneutral pH. J. Agric. food Chem.

Ubomba-Jaswa, E., Fernández-Ibáñez, P., Navntoft, C., Polo-López, M.I., McGuigan, K.G., 2010. Investigating the microbial inactivation efficiency of a 25L batch solar disinfection (SODIS) reactor enhanced with a compound parabolic collector (CPC) for household use. J. Chem. Technol. Biotechnol. 85, 1028–1037. https://doi.org/10.1002/jctb.2398.

Villegas- Guzman, P., Giannakis, S., Rtimi, S., Grandjean, D., Bensimon, M., de Alencastro, L.F., Torres-Palma, R., Pulgarin, C., 2017. A green solar photo-Fenton process for the elimination of bacteria and micropollutants in municipal wastewater treatment using mineral iron and natural organic acids. Appl. Catal. B Environ. 219, 538–549. https://doi.org/10.1016/j.apcatb.2017.07.066.

Viollier, E., Inglett, P., Hunter, K., Roychoudhury, A., Van Cappellen, P., 2000. The ferrozine method revisited: fe(II)/Fe(III) determination in natural waters. Appl. Geochemistry 15, 785–790. https://doi.org/10.1016/S0883-2927(99)00097-9.

Wegelin, M., Canonica, S., Mechsner, K., Fleischmann, T., Pesaro, F., Metzler, A., 1994. Solar water disinfection: scope of the process and analysis of radiation experiments. Aqua J. Water Supply Res. Technol. 43, 154–169.

WHO/UNICEF, 2015. Progress On Sanitation and Drinking Water. UNICEF and World Health Organization, Geneva.

World Health Organisation, 2007. pH in drinking-water. Guidel. Drink. water Qual. 2, 1–7.